J|A|C|S ARTICLES

Published on Web 03/29/2010

Excited State Distortion in Photochromic Ruthenium Sulfoxide Complexes

Beth Anne McClure, Eric R. Abrams, and Jeffrey J. Rack*

Department of Chemistry and Biochemistry, Nanoscale and Quantum Phenomena Institute, Ohio University, Athens, Ohio 45701

Received November 24, 2009; E-mail: rackj@ohio.edu

Abstract: A series of photochromic ruthenium sulfoxide complexes of the form $[Ru(bpy)_2(OSOR)]^+$, where bpy is 2,2′-bipyridine and OSOR is 2-(benzylsulfinyl)benzoate (OSOBn), 2-(napthalen-2-yl-methylsulfinyl)-benzoate (OSONap), or 2-(pentafluorophenylmethanesulfinyl)benzoate ($OSOBnF_5$), have been synthesized and characterized. In aggregate, the data are consistent with phototriggered isomerization of the sulfoxide from S-bonded to O-bonded. The S-bonded complexes feature ^{3}MLCT absorption maxima at 388 nm (R = BnF_5), 396 nm (R = Bn), and 400 nm (R = Nap). Upon charge transfer excitation the S-bonded peak diminishes concomitant with new peaks growing in at ∼350 and ∼495 nm. Spectroscopic and electrochemical data suggest that the electronic character of the substituent on the sulfur affects the properties of the S-bonded complexes, but not the O-bonded complexes. The isomerization is reversible in methanol solutions and, in the absence of light, thermally reverts to the S-bonded isomer with biexponential kinetics. The quantum yields of isomerization ($\Phi_{s\rightarrow o}$) were found to be 0.32, 0.22, and 0.16 for the R = BnF_5, Bn, and Nap complexes, respectively. Kinetic analyses of femtosecond transient absorption data were consistent with a nonadiabatic mechanism in which isomerization occurs from a thermally relaxed ^{3}MLCT state of S-bonded (or η^2-sulfoxide) character directly to the singlet O-bonded ground state. The time constants of isomerization ($\tau_{s\rightarrow o}$) were found to be 84, 291, and 427 ps for the R = BnF_5, Bn, and Nap complexes, respectively. Analysis of room temperature absorption and 77 K emission spectra reveal significant distortion between the S-bonded ground state (^1GS_S) and singlet metal-to-ligand charge transfer state ($^1MLCT_S$) and thermally relaxed ^{3}MLCT, respectively. The distortion is primarily attributed to low frequency metal−ligand and S═O vibrational modes, which are intrinsically involved in the isomerization pathway.

Introduction

Photoswitchable molecules which can be converted between two or more optically and electronically distinct states may be used for applications in logic gates,[1−3] molecular switches,[4−10] and other photoresponsive materials.[11−20] Although rotaxanes[4−9] and certain transition metal complexes featuring ambidentate ligands[21−24] may be triggered electrochemically by oxidation or reduction, light is a preferred trigger to induce rapid switching between states. Ideal characteristics of these complexes include efficient conversion of photonic energy into potential energy and a sufficiently long-lived metastable state. Our investigations of photoswitchable complexes have focused on a class of simultaneously electrochromic and photochromic ruthenium

(1) Andreasson, J.; Straight, S. D.; Bandyopdhyay, S.; Mitchell, R. H.; Moore, T. A.; Moore, A. L.; Gust, D. *Angew. Chem., Int. Ed.* **2007**, *46*, 958–961.
(2) Andreasson, J.; Straight, S. D.; Moore, T. A.; Moore, A. L.; Gust, D. *J. Am. Chem. Soc.* **2008**, *130*, 11122–11128.
(3) Straight, S. D.; Liddell, P. A.; Terazono, Y.; Moore, T. A.; Moore, A. L.; Gust, D. *Adv. Funct. Mater.* **2007**, *17*, 777–785.
(4) McNitt, K. A.; Parimal, K.; Share, A. I.; Fahrenbach, A. C.; Witlicki, E. H.; Pink, M.; Bediako, D. K.; Plaiser, C. L.; Le, N.; Heeringa, L. P.; Vander Griend, D. A.; Flood, A. H. *J. Am. Chem. Soc.* **2009**, *131*, 1305–1313.
(5) Periyasamy, G.; Sour, A.; Collin, J.-P.; Sauvage, J.-P.; Remacle, F. *J. Phys. Chem. B* **2009**, *113*, 6219–6229.
(6) Silvi, S.; Venturi, M.; Credi, A. *J. Mater. Chem.* **2009**, *19*, 2279–2294.
(7) Spruell, J. M.; Paxton, W. F.; Olsen, J.-C.; Benitez, D.; Tkatchouk, E.; Stern, C. L.; Trabolsi, A.; Friedman, D. C.; Goddard, W. A.; Stoddart, J. F. *J. Am. Chem. Soc.* **2009**, *131*, 11571–11580.
(8) Stoddart, J. F. *Chem. Soc. Rev.* **2009**, *38*, 1802–1820.
(9) Bonnet, S.; Collin, J.-P.; Koizumi, M.; Mobian, P.; Sauvage, J.-P. *Adv. Mater.* **2006**, *18*, 1239–1250.
(10) Irie, M. *Chem. Rev.* **2000**, *100*, 1685–1716.
(11) Dieckmann, V.; Eicke, S.; Rack, J. J.; Woike, T.; Imlau, M. *Opt. Express* **2009**, *17*, 15052–15060.
(12) Schaniel, D.; Imlau, M.; Weisemoeller, T.; Woike, T.; Kramer, K. W.; Gudel, H.-U. *Adv. Mater.* **2007**, *19*, 723–726.
(13) Yildiz, I.; Deniz, E.; Raymo, F. M. *Chem. Soc. Rev.* **2009**, *38*, 1859–1867.
(14) Imlau, M.; Schieder, R.; Rupp, R. A.; Woike, T. *Appl. Phys. Lett.* **1999**, *75*, 16–18.
(15) Imlau, M.; Woike, T.; Schieder, R.; Rupp, R. A. *Europhys. Lett.* **2001**, *53*, 471–477.
(16) Schefer, J.; Schaniel, D.; Petricek, V.; Woike, T. *Z. Kristallogr.* **2008**, *223*, 259–264.
(17) Woike, T.; Schaniel, D. *Z. Kristallogr.* **2008**, *223*, IV.
(18) Roberts, M. N.; Carling, C.-J.; Nagle, J. K.; Branda, N. R.; Wolf, M. O. *J. Am. Chem. Soc.* **2009**, *131*, 16644–16645.
(19) Roberts, M. N.; Nagle, J. K.; Finden, J. G.; Branda, N. R.; Wolf, M. O. *Inorg. Chem.* **2009**, *48*, 19–21.
(20) Irie, M.; Kobatake, S.; Horichi, M. *Science* **2001**, *291*, 1769–1772.
(21) Hamaguchi, T.; Inoue, Y.; Ujimoto, K.; Ando, I. *Polyhedron* **2008**, *27*, 2031–2034.
(22) Johansson, O.; Johannissen, L. O.; Lomoth, R. *Chem.—Eur. J.* **2009**, *15*, 1195–1204.
(23) Bitterwolf, T. E. *Coord. Chem. Rev.* **2006**, *250*, 1196–1207.
(24) Coppens, P.; Novozhilova, I.; Kovalevsky, A. *Chem. Rev.* **2002**, *102*, 861–883.

10.1021/ja9099399

Scheme 1. S-Bonded $[Ru(bpy)_2(OSOR)]^+$ Isomerizes to the Metastable O-Bonded Isomer upon Charge Transfer Irradiation[a]

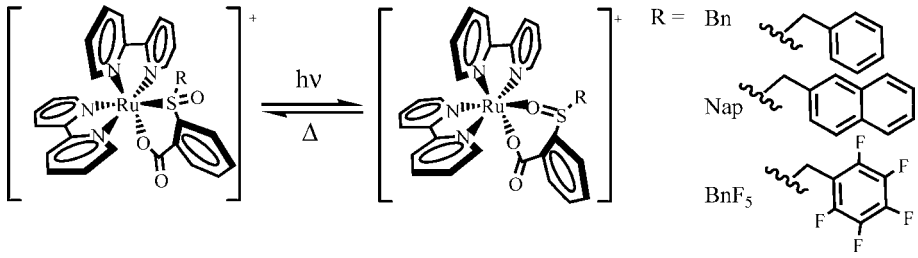

[a] The O-bonded metastable isomer reverts thermally to the S-bonded isomer.

polypyridine sulfoxide complexes, which exhibit phototriggered switching on the nanosecond to picosecond time scale.[25−38] The sulfoxide is S-bonded in the ground state and is switched to a metastable O-bonded state upon either charge transfer irradiation or oxidation of the ruthenium metal (Scheme 1).[36] The dramatic change in color arises from the difference in Ru−S and Ru−O bonding.

As exemplified by rhodopsin, which undergoes *cis*−*trans* isomerization with a time constant of 200 fs, a fast rate of isomerization is due to efficient relaxation via vibrational modes that lead directly to the photoproduct.[39−42] Many such reactions, including the conversion of $[RuCl_5(NO)]^{2-}$ to one of two metastable states (O-bonded or η^2-NO), have been proposed to occur via rapid nonradiative decay through conical intersections involving two or more reaction coordinates between adjacent potential energy surfaces.[43,44] Although these transitions are traditionally considered forbidden, higher order (e.g., spin orbit, rotational modes) and nonadiabatic coupling mechanisms increase the transition probability at the nuclear coordinates of the conical intersection, allowing for transitions to occur within a few vibrations.[45−49] Furthermore, dynamics are more effectively described by the shape and properties of the potential energy surfaces,[45,50] suggesting that they are strongly influenced by subtle structural modifications, solvent, or temperature.

As suggested by the work of McCusker and Damrauer,[51−53] $[Ru(bpy)_3]^{2+}$ (bpy = 2,2′-bipyridine) type complexes exhibit rapid localization from the singlet metal-to-ligand charge transfer (^{1}MLCT) state to the ^{3}MLCT excited state within ∼300 fs with unit quantum efficiency due to a large spin orbit coupling constant. Thus intramolecular vibrational relaxation, internal conversion, and intersystem crossing occur simultaneously. However, unlike photochromic complexes which feature large excited state displacement of nuclear coordinates, complexes like $[Ru(bpy)_3]^{2+}$ exhibit minimal displacement between the Franck−Condon and thermally relaxed ^{3}MLCT state geometries. Thus we raise the question of whether similar electronic factors, such as a large spin−orbit coupling constant, increase the probability of transition to a metastable state through conical intersections, thereby increasing the efficiency of phototriggered isomerization in ruthenium polypyridine complexes. The present work aims to analyze spectral properties of a series of photochromic complexes in an attempt to establish a relationship between the distortion energy of the ^{3}MLCT and isomerization reactivity. Furthermore, we hope to probe the effect of changing the electronic and steric factors contributing to excited state isomerization by variation of the substituent on the sulfur.

Experimental Section

Materials. The compound *cis*-$[Ru(bpy)_2Cl_2]\cdot 2H_2O$ was synthesized according to a published method.[54] The reagents $RuCl_3\cdot xH_2O$ and silver hexafluorophosphate ($AgPF_6$) were purchased from Strem and used as received. The reagents $[Ru(bpy)_3]Cl_2\cdot 6H_2O$, 2,2′-bipyridine (bpy), thiosalycylic acid, *m*-chloroperoxybenzoic acid, triethylamine, benzyl bromide, 2,3,4,5,6-pentafluorobenzyl bromide, 2-(bromomethyl)-napthalene, sodium hydroxide, and concentrated hydrochloric acid were purchased from Aldrich and used as received. All solvents such as methanol, ethanol, diethyl ether,

(25) Butcher, D. P.; Rachford, A. A.; Petersen, J. L.; Rack, J. J. *Inorg. Chem.* **2006**, *45*, 9178–9180.
(26) McClure, B. A.; Mockus, N. V.; Butcher, D. P.; Lutterman, D. A.; Turro, C.; Petersen, J. L.; Rack, J. J. *Inorg. Chem.* **2009**, *48*, 8084–8091.
(27) Mockus, N. V.; Petersen, J. L.; Rack, J. J. *Inorg. Chem.* **2006**, *45*, 8–10.
(28) Mockus, N. V.; Rabinovich, D.; Petersen, J. L.; Rack, J. J. *Angew. Chem., Int. Ed.* **2008**, *47*, 1458–1461.
(29) Rachford, A. A.; Petersen, J. L.; Rack, J. J. *Inorg. Chem.* **2005**, *44*, 8065–8075.
(30) Rachford, A. A.; Petersen, J. L.; Rack, J. J. *Inorg. Chem.* **2006**, *45*, 5953–5960.
(31) Rachford, A. A.; Rack, J. J. *J. Am. Chem. Soc.* **2006**, *128*, 14318–14324.
(32) Rack, J. J.; Mockus, N. V. *Inorg. Chem.* **2003**, *42*, 5792–5794.
(33) Rack, J. J.; Rachford, A. A.; Shelker, A. M. *Inorg. Chem.* **2003**, *42*, 7357–7359.
(34) Rack, J. J.; Winkler, J. R.; Gray, H. B. *J. Am. Chem. Soc.* **2001**, *123*, 2432–2433.
(35) Rack, J. J. *Z. Kristallogr.* **2008**, *223*, 356–362.
(36) Rack, J. J. *Coord. Chem. Rev.* **2009**, *253*, 78–85.
(37) Mockus, N. V.; Marquard, S.; Rack, J. J. *J. Photochem. Photobiol. A* **2008**, *200*, 39–43.
(38) McClure, B. A.; Rack, J. J. *Angew. Chem., Int. Ed.* **2009**, *48*, 8556–8558.
(39) Kim, J. E.; McCamant, D. W.; Zhu, L.; Mathies, R. A. *J. Phys. Chem. B* **2001**, *105*, 1240–1249.
(40) Mathies, R. A.; Cruz, C. H. B.; Pollard, W. T.; Shank, C. V. *Science* **1988**, *240*, 777–779.
(41) Peteanu, L. A.; Schoenlein, R. W.; Wang, Q.; Mathies, R. A.; Shank, C. V. *Proc. Natl. Acad. Sci. U.S.A.* **1993**, *90*, 11762–11766.
(42) Schoenlein, R. W.; Peteanu, L. A.; Mathies, R. A.; Shank, C. V. *Science* **1991**, *254*, 412–415.
(43) Baranovskii, V. I.; Sizova, O. V. *J. Struct. Chem.* **2008**, *49*, 803–809.
(44) Levine, B. G.; Martinez, T. J. *Annu. Rev. Phys. Chem.* **2007**, *58*, 613–634.
(45) Domcke, W.; Yarkony, D. R.; Koppel, H. *Conical Intersections: Electronic Structure, Dynamics and Spectroscopy*; World Scientific: Singapore, 2004; Vol. 15.
(46) Barckholtz, T. A.; Miller, T. A. *Int. Rev. Phys. Chem.* **1998**, *17*, 435–524.
(47) Matsika, S.; Yarkony, D. R. *J. Chem. Phys.* **2002**, *116*, 2825–2835.
(48) Mayer, M.; Cederbaum, L. S. *J. Chem. Phys.* **1996**, *105*, 4938–4963.
(49) Worth, G. A.; Cederbaum, L. S. *Annu. Rev. Phys. Chem.* **2004**, *55*, 127–58.
(50) Klessinger, M.; Michl, J. *Excited States and Photochemistry of Organic Molecules*; VCH: New York, 1995.
(51) Damrauer, N. H.; Cerullo, G.; Yeh, A.; Boussie, T. R.; Shank, C. V.; McCusker, J. K. *Science* **1997**, *275*, 54–57.
(52) Damrauer, N. H.; McCusker, J. K. *J. Phys. Chem. A* **1999**, *103*, 8440–8446.
(53) McCusker, J. K. *Acc. Chem. Res.* **2003**, *36*, 876–887.
(54) Sullivan, B. P.; Salmon, D. J.; Meyer, T. J. *Inorg. Chem.* **1978**, *17*, 3334–3341.

dichloromethane, chloroform, acetonitrile, and hexanes were purchased from VWR and used without further purification. Tetrabutylammonium hexafluorophosphate ($TBAPF_6$) was purchased from Aldrich and recrystallized three times from hot ethanol. Acetonitrile for electrochemical experiments was HPLC grade (Burdick and Jackson) and used without further purification. The synthesis and isolation of all ruthenium sulfoxide complexes were carried out in the dark or under red light.

2-Benzylsulfanyl-benzoic Acid (OSBn). Thiosalicylic acid (2.992 g, 19.4 mmol) and 2 equiv of sodium hydroxide (1.578 g, 39.4 mmol) were combined in methanol (75 mL). The solution was stirred at room temperature for 10 min until a yellow solution formed and the solids were dissolved. The methanol was removed by rotorary evaporation yielding a light yellow solid. Acetone (100 mL) and benzyl bromide (2.53 mL, 21.3 mmol) were added to the resulting solid. A white precipitate immediately formed upon mixing, and the solution was sonicated for 5 min and then placed in a −4 °C freezer for 1 h. The white precipitate was collected and washed three times with cold diethyl ether. The resulting white solid was dissolved in water (100 mL), and concentrated HCl was added (1.8 mL) to yield a white precipitate. After being placed in a −4 °C freezer for 1 h, the precipitate was collected by vacuum filtration and washed with cold water. The white solid was then dried under vacuum overnight. Yield: 4.260 g (89.9%). ^{1}H NMR (d^6-acetone, 300 MHz) δ: 8.05 (d, 1H), 7.52 (m, 4H), 7.27 (m, 4H), 4.27 (s, 2H) ppm.

2-(Naphthalen-2-ylmethylsulfanyl)-benzoic Acid (OSNap). OSNap was synthesized by following a similar procedure as OSBn, starting with thiosalicylic acid (0.701 g, 4.55 mmol) and using 2-(bromomethyl)naphthalene (1.067 g, 4.83 mmol) in place of the benzyl bromide. Yield: 0.565 g (42.2%). ^{1}H NMR (d^6-acetone, 300 MHz) δ: 8.00 (d, 1 H), 7.98 (t, 1 H), 7.87 (m, 3 H), 7.60 (m, 2 H), 7.48 (m, 3 H), 7.21 (m, 1 H), 4.40 (s, 2 H) ppm.

2-Pentafluorophenylmethylsulfanyl-benzoic Acid ($OSBnF_5$). $OSBnF_5$ was synthesized in a similar procedure to that for OSBn, starting with thiosalicylic acid (1.015 g, 6.583 mmol) and substituting 2,3,4,5,6-pentafluorobenzyl bromide for the benzyl bromide. Yield: 1.434 g (65.4%). ^{1}H NMR (d^6-acetone, 300 MHz) δ: 7.98 (d, 1 H), 7.60 (m, 2 H), 7.35 (m, 1 H), 4.33 (s, 2 H) ppm.

2-Pentafluorophenylmethanesulfinyl-benzoic Acid ($OSOBnF_5$). The compound $OSBnF_5$ (172 mg, 0.515 mmol) was dissolved in 35 mL of chloroform. In a separate 35 mL of chloroform, *m*-chloroperoxybenzoic acid (150 mg 60% peroxo reagent by ^{1}H NMR, 0.521 mmol) was dissolved and added slowly to the $OSBnF_5$ solution. The combined solutions were stirred at room temperature for 10 min. The solvent was removed by rotary evaporation. Approximately 2 mL of diethyl ether were added to the resulting residue, and the solid was isolated by vacuum filtration and air-dried. Yield: 111 mg (62%). ^{1}H NMR (d^6-acetone, 300 MHz) δ: 8.21 (d, 1 H), 7.66−7.80 (m, 3 H), 4.68 (d, 1 H), 4.40 (d, 1 H) ppm.

$[Ru(bpy)_2(OSBn)](PF_6)$. The complex *cis*-$[Ru(bpy)_2Cl_2]$ (197 mg, 0.379 mmol), OSBn (142 mg, 0.580 mmol), silver hexafluorophosphate (211 mg, 0.835 mmol), and triethylamine (150 μL) were dissolved in 100 mL of ethanol and refluxed for 6 h under nitrogen. The solution changed from a deep purple to a red color. The solution was cooled to −30 °C overnight to ensure complete precipitation of AgCl. The AgCl was filtered off and rinsed with acetone until the filtrate was colorless. Solvent was removed by rotary evaporation. The resulting residue was dissolved in a minimal amount of ethanol and acetone. Hexanes were added to precipitate a red-orange solid. The solid was isolated in an approximately quantitative yield via vacuum filtration and washed with hexanes and air-dried. UV−vis (MeOH) λ_{max} = 458 nm (5900 M^{-1} cm^{-1}). $E^{\circ\prime}$ $Ru^{3+/2+}$ vs Ag/Ag^+ (CH_3CN) = 0.61 V. ^{1}H NMR (d^6-acetone, 300 MHz) δ: 9.61 (d, 1 H), 8.82 (d, 1 H), 8.68 (d, 1 H), 8.55 (m, 3 H), 8.37 (t, 1 H), 8.24 (d, 1 H), 8.00 (m, 4 H), 7.76 (d, 1 H), 7.56 (d, 1 H), 7.40 (m, 3 H), 7.25 (m, 3 H), 7.13 (t, 1 H), 7.00 (t, 2 H), 6.67 (d, 2 H), 3.92 (d, 1 H), 3.40 (d, 1 H) ppm.

$[Ru(bpy)_2(OSOBn)](PF_6)\cdot 0.75H_2O$ (OSOBn is 2-Benzylsulfinyl-benzoic Acid). The complex $[Ru(bpy)_2(OSBn)](PF_6)$ (101 mg, 0.124 mmol) and 60% *m*-chloroperoxybenzoic acid (57 mg, 0.199 mmol) were dissolved in 50 mL of dichloromethane and stirred at room temperature for 25 h. The solvent was removed by rotary evaporation, and the resulting residue was dissolved in a minimum amount of methanol. Ether was added to precipitate the ruthenium solid. The solid was isolated by vacuum filtration, rinsed with ether, and air-dried. Yield: 86 mg (83%). UV−vis (MeOH) λ_{max} = 396 nm (6200 M^{-1} cm^{-1}) S-bonded, 350 nm (8000 M^{-1} cm^{-1}) and 496 nm (7800 M^{-1} cm^{-1}) O-bonded. ν(S=O) = 1097 cm^{-1} (S-bonded), 1022 cm−1 (O-bonded). $E^{\circ\prime}$ $Ru^{3+/2+}$ vs Ag/Ag^+ (CH_3CN) = 0.90 V S-bonded, 0.53 and 0.34 V O-bonded. ^{1}H NMR (d^6-acetone, 300 MHz) δ: 9.61 (d, 1 H), 8.82 (d, 1 H), 8.68 (d, 1 H), 8.55 (m, 3 H), 8.37 (t, 1 H), 8.24 (d, 1 H), 8.00 (m, 4 H), 7.76 (d, 1 H), 7.56 (d, 1 H), 7.40 (m, 3 H), 7.25 (m, 3 H), 7.13 (t, 1 H), 7.00 (t, 2 H), 6.67 (d, 2 H), 3.92 (d, 1 H), 3.40 (d, 1 H) ppm. Elemental analysis, calculated for $[Ru(C_{10}H_8N_2)_2(C_{14}H_{11}O_2S)]PF_6\cdot 0.75H_2O$: C, 49.12%; H, 3.46%; O, 7.22%; N, 6.74%. Found: C, 48.75%; H, 3.41%; O, 7.17%; N, 6.72%.

$[Ru(bpy)_2(OSNap)](PF_6)$. The complex *cis*-$[Ru(bpy)_2Cl_2]$ (151 mg, 0.291 mmol), OSNap (105 mg, 0.357 mmol), silver hexafluorophosphate (159 mg, 0.629 mmol), and triethylamine (100 μL) were dissolved in 50 mL of ethanol and refluxed under nitrogen for 18 h. The solution was cooled to −30 °C to ensure complete precipitation of AgCl. The AgCl was filtered off and rinsed with acetone until the filtrate was colorless. Solvent was removed by rotary evaporation. The resulting residue was dissolved in a minimal amount of ethanol. Hexanes were added to precipitate a red-orange solid. The solid was isolated in via vacuum filtration and washed with hexanes and air-dried. Yield: 241 mg (97%). UV−vis (MeOH) λ_{max} = 456 nm (6700 M^{-1} cm^{-1}). $E^{\circ\prime}$ $Ru^{3+/2+}$ vs Ag/Ag^+ (CH_3CN) = 0.61 V. ^{1}H NMR (d^6-acetone, 300 MHz) δ: 9.64 (d, 1 H), 8.87 (d, 1 H), 8.58 (m, 2 H), 8.46 (d, 1 H), 8.27 (m, 3 H), 8.05 (m, 3 H), 7.81 (m, 3 H), 7.40 (m, 10 H), 7.17 (t, 1 H), 7.07 (s, 1 H), 6.90 (d, 1 H), 4.15 (d, 1 H), 3.68 (d, 1 H) ppm.

$[Ru(bpy)_2(OSONap)](PF_6)\cdot H_2O$ (OSONap is 2-(Naphthalen-2-ylmethylsulfinyl)-benzoic Acid). The complex $[Ru(bpy)_2(OSNap)](PF_6)$ (88 mg, 0.101 mmol) and 60% *m*-chloroperoxybenzoic acid (45 mg, 0.155 mmol) were dissolved in 30 mL of dichloromethane and stirred at room temperature for 24 h. The solvent was removed by rotary evaporation, and the resulting residue was dissolved in a minimum amount of methanol. Ether was added to induce precipitation. The solid was isolated by vacuum filtration, rinsed with ether, and air-dried. Yield: 84 mg (94%). UV−vis (MeOH) λ_{max} = 400 nm (6900 M^{-1} cm^{-1}) S-bonded, 351 nm (8600 M^{-1} cm^{-1}) and 496 nm (8600 M^{-1} cm^{-1}) O-bonded. ν(S=O) = 1093 cm^{-1} (S-bonded), 1022 cm^{-1} (O-bonded). $E^{\circ\prime}$ $Ru^{3+/2+}$ vs Ag/Ag^+ (CH_3CN) = 0.90 V S-bonded, 0.53 V and 0.34 V O-bonded. ^{1}H NMR (d^6-acetone, 300 MHz) δ: 9.52 (d, 1 H), 9.03 (d, 1 H), 8.71 (m, 2 H), 8.61 (d, 1 H), 8.53 (d, 1 H), 8.44 (t, 1 H), 8.22 (m, 1 H), 8.10 (m, 4 H), 7.95 (d, 1 H), 7.80 (d, 1 H), 7.54 (m, 8 H), 7.37 (t, 1 H), 7.27 (d, 2 H), 7.17 (s, 1 H), 6.74 (d, 1 H), 4.51 (d, 1 H), 4.20 (d, 1 H) ppm. Elemental analysis, calculated for $[Ru(C_{10}H_8N_2)_2(C_{18}H_{13}O_3S)]PF_6\cdot H_2O$: C, 51.50%; H, 3.53%; O, 7.22%; N, 6.33%. Found: C, 51.42%; H, 3.21%; O, 6.93%; N, 6.34%.

$[Ru(bpy)_2(OSOBnF_5)](PF_6)\cdot 1.2H_2O$. The complex *cis*-$[Ru(bpy)_2Cl_2]$ (56 mg, 0.108 mmol), $OSOBnF_5$ (45 mg, 0.129 mmol), silver hexafluorophosphate (59 mg, 0.234 mmol), and triethylamine (50 μL) were dissolved in 25 mL of ethanol and refluxed under nitrogen for 19 h. The solution was cooled to −30 °C overnight to ensure complete precipitation of AgCl. The AgCl was filtered off by vacuum filtration and rinsed with acetone. Solvent was removed by rotary evaporation. The resulting solid was dissolved in dichloromethane and extracted with a 10 mL aqueous solution of 22 mg of $LiOH\cdot H_2O$ to remove NEt_3HPF_6 formed during reaction. The dichloromethane layer was dried with magnesium sulfate, and the solvent was removed by rotary evaporation. The solid was dissolved in ∼2 mL ethanol. Ether was

added to precipitate a yellow solid. The product was isolated via vacuum filtration, washed with ether (3 × 15 mL), and air-dried. Yield: 80 mg (82%). UV−vis (MeOH) λ_{max} = 388 nm (5970 M^{-1} cm^{-1}) S-bonded, 350 nm (7800 M^{-1} cm^{-1}) and 495 nm (7900 M^{-1} cm^{-1}) O-bonded. ν(S═O) = 1105 cm^{-1} (S-bonded), 1022 cm^{-1} (O-bonded). $E^{o\prime}$ $Ru^{3+/2+}$ vs Ag/Ag^+ (CH_3CN) = 0.97 V S-bonded, 0.53 V O-bonded. ^{1}H NMR (d^6-acetone, 300 MHz) δ: 9.50 (d, 1 H), 9.02 (d, 1 H), 8.88 (d, 1 H), 8.79 (d, 1 H), 8.72 (d, 1 H), 8.60 (m, 2 H), 8.22 (t, 1 H), 8.12 (m, 4 H), 7.98 (d, 1 H), 7.73 (d, 1 H), 7.61 (m, 3 H), 7.49 (m, 2 H), 7.38 (t, 1 H), 4.40 (d, 1 H), 3.98 (d, 1 H) ppm. Elemental analysis, calculated for $[Ru(C_{10}H_8N_2)_2(C_{14}H_7O_3SF_5)]PF_6 \cdot 1.2\ H_2O$: C, 43.94%; H, 2.65%; N, 6.03%; S, 3.45%. Found: C, 43.58%; H, 2.84%; N, 6.38%; S, 3.61%.

[Ru(bpy)$_2$(OSBnF$_5$)](PF$_6$). The synthesis and isolation of this complex were similar to those for $[Ru(bpy)_2(OSOBnF_5)](PF_6)$. The complex *cis*-$[Ru(bpy)_2Cl_2]$ (224 mg, 0.431 mmol), $OSBnF_5$ (160 mg, 0.479 mmol), silver hexafluorophosphate (220 mg, 0.870 mmol), and triethylamine (150 μL) were dissolved in 100 mL of ethanol and refluxed under nitrogen for 4.5 h. The isolation and purification of the product were carried out as described above. Yield: 87 mg (23%). UV−vis (MeOH) λ_{max} = 448 nm (6500 M^{-1} cm^{-1}). $E^{o\prime}$ $Ru^{3+/2+}$ vs Ag/Ag^+ (CH_3CN) = 0.67 V. ^{1}H NMR (d^6-acetone, 300 MHz) δ: 9.66 (d, 1 H), 8.92 (d, 1 H), 8.72 (t, 2 H), 8.62 (t, 2 H), 8.48 (t, 1 H), 8.26 (d, 1 H), 8.10 (m, 4 H), 7.87 (d, 1 H), 7.70 (d, 1 H), 7.46 (m, 3 H), 7.29 (m, 3 H), 4.08 (d, 1 H), 2.94 (d, 1 H) ppm.

Instrumentation. Cyclic voltammetry was performed on a CH Instruments CHI 730A Electrochemical Analyzer. This workstation contains a digital simulation package as part of the software package to operate the workstation (CHI version 2.06). The working electrode was either a glassy carbon disk (Cypress Systems, 1.5 mm) or platinum (BAS, 2.0 mm) electrode. The counter and reference electrodes were Pt wire and Ag/Ag^+, respectively. Electrochemical measurements were performed in acetonitrile solutions containing 0.1 M $TBAPF_6$ electrolyte in a one-compartment cell.

Electronic absorption spectra were collected on an Agilent 8453 spectrophotometer. Bulk photolysis experiments were conducted using a 75 W xenon-arc lamp (Oriel) fitted with a Canon standard camera UV filter. Corrected emission measurements were collected at 77 K in 4:1 EtOH/MeOH solutions on a PTI-C60 fluorimeter equipped with a Hamamatsu R928 PMT(185−900 nm). Quantum yields of emission were determined using $[Ru(bpy)_3]Cl_2$ as a reference. Proton nuclear magnetic resonance (^{1}H NMR) spectra were collected on a 300 MHz Bruker spectrometer in deuterated chloroform ($CDCl_3$) or deuterated acetone (d^6-acetone). Infrared spectroscopic measurements were collected on a Nicolet 380 FT-IR spectrometer. Samples were prepared by evaporating a solution of dichloromethane onto a 25 mm × 4 mm KBr plate. The ν(S═O) stretch was assigned in the S-bonded isomer by comparison between the thioether and sulfoxide complexes. The O-bonded spectrum was achieved by irradiating the dichloromethane solution as described above before evaporating the solution onto a KBr plate.

Picosecond transient absorption spectra were acquired at the Ohio Laboratory for Kinetic Spectrometry (OLKS) as part of Bowling Green State University's (BGSU) Center for Photochemical Studies. The experimental details were described previously, and only a brief discussion is provided here.[55−57] Spectra-Physics Hurricane Evolution and Ti:sapphire were combined to yield 800 nm pulses of 130 fs in duration at a rate of 1 kHz. The excitation wavelength of 400 nm (~2 μJ/pulse) was obtained from frequency-doubling the Ti:sapphire fundamental. A portion of the 800 nm fundamental was employed to generate the white light continuum probe source by focusing the light through either a CaF_2 or 3 mm sapphire plate. Detection was achieved with a double CCD spectrograph over the range ~360−750 nm for CaF_2 or ~450−750 nm for sapphire. Transient spectra at a particular delay time represent the average of 4000 excitation pulses. The instrument is operated through an in-house (BGSU) LabVIEW software routine. Kinetic analysis of the data was performed at Ohio University (OU) with the SPECFIT (version 3.0.37, Spectrum Software Associates) program, a global analysis routine based on single value decomposition. Goodness-of-fit was evaluated qualitatively by inspection of the residual plots. For the S-bonded complex, samples were prepared in bulk methanol solution and analyzed using a flow through 2 mm path length cell with a flow rate of approximately 15−23 mL/s. For the O-bonded isomer, a 2 mm path length steady state cell containing a small portion of the same solution was used.

Quantum Yield of Isomerization. Quantum yield of isomerization measurements were obtained by irradiating solutions of the complexes $[Ru(bpy)_2(OSO\text{-}R)]^+$ in methanol at room temperature. Photolysis was achieved using a PTI C-60 fluorimeter. The wavelength of light was set to the lower energy isosbestic point between S-bonded and O-bonded isomers. The incident radiation intensity, I_o, was determined by potassium ferrioxalate actinometry. The quantum yield was determined according to eq 1 in a manner similar to that previously described for photosubstitution reactions.[29,58−61] In eq 1, C_T and C_p are the total concentration and concentration of O-bonded formed respectively, V is the volume of solution (3 mL), ϵ is the molar extinction coefficient at the isosbestic point, I_o is the incident radiation intensity, and l is the path length (1 cm). The concentration of O-bonded isomer was determined using multilinear regression analysis.

$$\Phi = \frac{C_T V[\ln(C_T) - \ln(C_T - C_p)]}{tI_o(1 - 10^{-\varepsilon C_T l})} \quad (1)$$

Results and Discussion

We have previously reported the synthesis and spectral properties of $[Ru(bpy)_2(OSO)]^+$, where OSO is 2-methanesulfinylbenzoate.[25,26] Analogous benzoate ligands (OS-R) have been synthesized from the common starting material thiosalicylic acid with benzyl bromide or 2-(bromomethyl)naphthalene. These ligands were subsequently allowed to react with $[Ru(bpy)_2Cl_2]$ in the presence of triethylamine and 2 equiv of $AgPF_6$ to yield the corresponding thioether coordination complexes in high yields. The thioether complexes were then oxidized to the corresponding sulfoxide complexes by reaction with *m*-chloroperoxybenzoic acid. The exception was the complex $[Ru(bpy)_2(OSOBnF_5)]^+$ which did not readily undergo oxidation from the thioether to the sulfoxide. Alternatively, the $OSBnF_5$ ligand was oxidized using *m*-chloroperoxybenzoic acid to yield the sulfoxide ligand, $OSOBnF_5$, which was subsequently allowed to react with $[Ru(bpy)_2Cl_2]$, triethylamine, and 2 equiv of $AgPF_6$ to yield $[Ru(bpy)_2(OSOBnF_5)]^+$. The synthesis of this complex also required an extraction with an aqueous LiOH solution to remove NEt_3HPF_6, which was not necessary with the complexes $[Ru(bpy)_2(OSBn)]^+$ or $[Ru(bpy)_2(OSNap)]^+$. The identity and formulation of the complexes was confirmed by ^{1}H NMR and IR spectroscopy and elemental analysis.

(55) Nikolaitchik, A. V.; Korth, O.; Rodgers, M. A. J. *J. Phys. Chem. A* **1999**, *103*, 7587–7596.
(56) Okhrimenko, A. N.; Gusev, A. V.; Rodgers, M. A. J. *J. Phys. Chem. A* **2005**, *109*, 7653–7656.
(57) Pelliccioli, A. P.; Henbest, K.; Kwag, G.; Carvagno, T. R.; Kenney, M. E.; Rodgers, M. A. J. *J. Phys. Chem. A* **2001**, *105*, 1757–1766.
(58) Bonnet, S.; Collin, J.-P.; Sauvage, J.-P.; Schofield, E. *Inorg. Chem.* **2004**, *43*, 8346–8354.
(59) Hecker, C. R.; Fanwick, P. E.; McMillin, D. R. *Inorg. Chem.* **1991**, *30*, 659–666.
(60) Kirchhoff, J. R.; McMillin, D. R.; Marnot, P. A.; Sauvage, J.-P. *J. Am. Chem. Soc.* **1985**, *107*, 1138–1141.
(61) Suen, H.-F.; Wilson, S. W.; Pomerantz, M.; Walsh, J. L. *Inorg. Chem.* **1989**, *28*, 786–791.

Table 1. Spectroscopic and Electrochemical Characterization for $[Ru(bpy)_2(OSOR)]^+$

	R		
	Bn	Nap	BnF_5
λ_{max} (S-bonded), nm (ϵ, M^{-1} cm^{-1})	396 (6220)	400 (6870)	388 (5970)
λ_{max} (O-bonded), nm (ϵ, M^{-1} cm^{-1})	496 (7820)	496 (8640)	495 (7890)
fwhm, cm^{-1}, S-bonded	7360	6380	7250
$\lambda_{max,em}$ (S-bonded), nm (Φ_{em}), 77 K	576 (0.076)	580 (0.090)	572 (0.034)
$E^{o\prime}$ (S-bonded), V	0.896	0.896	0.974
$E^{o\prime}$ (O-bonded), V[a]	0.525	0.528	0.533
	0.340	0.336	
ν(S=O), cm^{-1} (S-bonded)	1097	1093	1105
ν(S=O), cm^{-1} (O-bonded)	1022	1022	1022

[a] We have observed what appears to be two O-bonded isomers by cyclic voltammetry for the R = Bn and Nap complexes, but not for the R = BnF_5 complex. We are still investigating this result.

The ν(S=O) stretches for the S-bonded complexes (Table 1) agree well with literature values for other transition metal dimethylsulfoxide (dmso) complexes.[62,63] The electronic character of the substituent on sulfur appears to affect the ν(S=O) stretch with higher frequencies corresponding to the more electron-withdrawing groups. This is likely a through bond or inductive effect since the opposite trend would be expected for an enhancement of a π-back bonding interaction between the sulfoxide group and the ruthenium metal center. The O-bonded ν(S=O) stretches are somewhat higher than those listed in literature for O-bonded dmso complexes but do not show any variation with different substituents.

The absorption maxima of the lowest energy transition occur at 388 nm (R = BnF_5), 396 nm (R = Bn), and 400 nm (R = Nap) (Table 1) for the S-bonded isomers, which are in close agreement with the S-bonded isomer of the previously reported $[Ru(bpy)_2(OSO)]^+$ complex (λ_{max} = 396 nm). Therefore, this transition is assigned as an MLCT band of the S-bonded isomer for these complexes. As for $[Ru(bpy)_2(OSO)]^+$, there is a significant blue shift in the absorption maximum of the S-bonded sulfoxide complexes relative to the thioether complexes as well as $[Ru(bpy)_3]^{2+}$, indicative of stabilization of the ruthenium dπ orbitals.[64] This stabilization is mirrored in the shift in $Ru^{3+/2+}$ reduction potentials (Table 1). As evidenced by the similar absorption maxima and $Ru^{3+/2+}$ reduction potentials, the stabilization conferred in both the R = Bn and Nap complexes matches closely with that of $[Ru(bpy)_2(OSO)]^+$ in which the substituent on the sulfur is a methyl group (R = Me). This suggests that despite the steric bulk of these groups, the effect on the extent of Ru−S mixing, and therefore on the ground state electronic structure, is negligible. In contrast, the R = BnF_5 complex exhibits a dramatic blue shift in the absorption maximum for both the sulfoxide and thioether complexes (388 and 448 nm, respectively) relative to the corresponding R = Bn complexes (396 and 458 nm, respectively). This indicates that the electron-withdrawing fluorine atoms have an electronic effect at the metal center through the sulfur, despite the aliphatic methylene carbon connecting them. This electronic effect is consistent with the relatively more positive $Ru^{3+/2+}$ potentials observed for this complex as well.

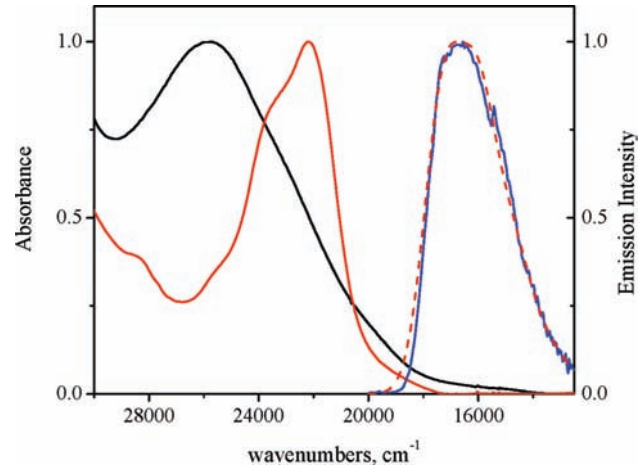

Figure 1. Absorption spectra of S-$[Ru(bpy)_2(OSOBnF_5)]^+$ (black) and $[Ru(bpy)_3]^{2+}$ (red) in methanol and normalized corrected 77 K emission of S-$[Ru(bpy)_2(OSOBnF_5)]^+$ in 4:1 EtOH/MeOH glass (experimental, blue; calculated fit, red dashed). Experimental and calculated emission of R = Bn and Nap and $[Ru(bpy)_3]^{2+}$ in Supporting Information.

The absorption spectra of these complexes are notably broader than the model complex $[Ru(bpy)_3]^{2+}$ (*fwhm* = 3550 cm^{-1}, MeOH) with full width at half-maximum (*fwhm*) values of 7360, 6380, and 7250 cm^{-1} for R = Bn, Nap, and BnF_5 (Figure 1), respectively. The *fwhm* values were obtained by doubling the difference (in cm^{-1}) between the peak maximum and the point at half of the maximum intensity on the low energy side. Previous studies have described the MLCT manifold of $[Ru(bpy)_3]^{2+}$ as a composite of four distinct transitions (d$\pi_{a1}\rightarrow\pi^*_{1a2}$, d$\pi_{a1}\rightarrow\pi^*_{1e}$, d$\pi_e\rightarrow\pi^*_{1a2}$, d$\pi_e\rightarrow\pi^*_{1e}$).[65,66] Due to the pseudo-C_2 reduced symmetry of our complexes, the d$\pi_e\rightarrow\pi^*_e$ transitions will be further split, yielding more transitions. Despite this, TD-DFT calculations of $[Ru(bpy)_2(OSO)]^+$ have found closely spaced transitions at 422 nm (f = 0.0625) and 379 nm (f = 0.0623) which overlap in solution to give a single band with a peak at 396 nm, which we have assigned as a d$\pi\rightarrow\pi^*$ transition.[26] For simplicity we have chosen to treat the spectra of $[Ru(bpy)_3]^{2+}$ and $[Ru(bpy)_2(OSOR)]^+$ as a single transition (see below). While this approach may overestimate the width of the bands, it will at least provide a qualitative comparison of the compounds.

The *fwhm* is proportional to the nuclear displacement (ΔQ) between the equilibrium geometries of the ground state (^{1}GS) and the ^{1}MLCT state.[67] The distortion or reorganization energy (λ^*, Scheme 2) is proportional to *fwhm* squared and is typically classified into outer sphere or solvent (λ_o), intraligand (λ_{IL}), and metal−ligand (λ_{ML}) contributions as described in eq 2, in which $h\nu_{IL}$ and $h\nu_{ML}$ are intraligand (bpy ring modes) and metal−ligand vibrational (Ru−N, Ru−S and Ru−O) modes, respectively.[67,68] The values for λ_o and λ_{IL} are expected to be similar to those for $[Ru(bpy)_3]^{2+}$, whereas λ_{ML} should be greater due to the change in bonding ligation in isomerizable compounds. Assuming approximate values of 500, 1350, 1300, and 500 cm^{-1} for λ_o, λ_{IL}, $h\nu_{IL}$, and $h\nu_{ML}$, respectively, based on results for $[Ru(bpy)_3]^{2+}$ and other ruthenium polypyridine complexes,[65,68]

(62) Alessio, E. *Chem. Rev.* **2004**, *104*, 4203–4242.
(63) Calligaris, M. *Coord. Chem. Rev.* **2004**, *248*, 351–375.
(64) Lutterman, D. A.; Rachford, A. A.; Rack, J. J.; Turro, C. *J. Phys. Chem. A* **2009**, *113*, 11002–11006.
(65) Kober, E. M.; Meyer, T. J. *Inorg. Chem.* **1984**, *23*, 3877–3886.
(66) Kober, E. M.; Meyer, T. J. *Inorg. Chem.* **1982**, *21*, 3967–3977.
(67) Solomon, E. I.; Lever, A. B. P. *Inorganic Electronic Structure and Spectroscopy*; John Wiley & Sons: New York, 1999.
(68) Winkler, J. R.; Netzel, T. L.; Creutz, C.; Sutin, N. *J. Am. Chem. Soc.* **1987**, *109*, 2381–2392.

Scheme 2. Potential Energy Surfaces for Ground State (^{1}GS), ^{1}MLCT, and ^{3}MLCT[a]

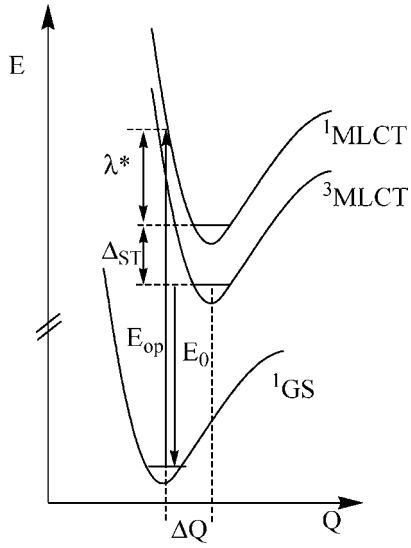

[a] E_{op} is optical energy for MLCT transition, E_0 is the difference between zeroth vibrational levels of ^{1}GS and ^{3}MLCT, and Δ_{ST} is singlet−triplet energy splitting, λ^* is distortion energy between ^{1}GS and ^{1}MLCT.

eq 2 predicts the metal−ligand contribution λ_{ML} to be 10 800, 14 400, and 14 800 cm^{-1} for R = Nap, BnF_5, and Bn, respectively. By this analysis the metal−ligand contribution is clearly the dominant mode of distortion. The values of E_0, the zero−zero energy, may be calculated from $E_0 = E_{op} - \lambda^* - \Delta_{ST}$, where E_{op} is the optical absorption maximum; λ^* is the sum of λ_o, λ_{IL}, and λ_{ML}; and Δ_{ST} is the triplet−singlet energy gap (3000 cm^{-1}) as reported for $[Ru(bpy)_3]^{2+}$,[66,68] to yield values of 9350, 6520, and 5600 cm^{-1} for R = Nap, BnF_5, and Bn, respectively. The E_0 values correspond to approximate emission maxima at wavelengths of 1070, 1530, and 1780 nm for R = Nap, BnF_5, and Bn, respectively. No emission was observed for these complexes at room temperature over the range 500−850 nm, and further measurements are needed to see if there is emission in the NIR. However, the calculated values are significantly red-shifted from the emission maxima (λ_{em}) observed at 77 K with values of 580, 576, and 572 nm for R = Nap, Bn, and BnF_5, respectively. For comparison, our analysis of $[Ru(bpy)_3]^{2+}$ yields values of $\lambda_{ML} = 510$ cm^{-1}, $E_0 = 16\,860$ cm^{-1}, and $\lambda_{em} = 590$ nm, which agree reasonably well with previously reported values of $\lambda_{ML} = 500$ cm^{-1} and $\lambda_{em} = 620$ nm (16 130 cm^{-1}), thus validating our single transition approximation employed in this approach.[68,69] This analysis shows that the low frequency metal−ligand vibrations strongly affect the appearance of the absorption spectrum and that the potential energy surfaces are sensitive to temperature.

$$\frac{(fwhm)^2}{5.55} = \lambda_o(2kT) + \lambda_{ML}\left(h\nu_{ML}\coth\left(\frac{h\nu_{ML}}{2kT}\right)\right) + \lambda_{IL}(h\nu_{IL}) \quad (2)$$

Upon charge transfer irradiation, the absorption peak near 400 nm diminishes in intensity concomitant with a growth in absorption near ~350 and ~495 nm (Table 1). These features are consistent with other $Ru(bpy)_2$ complexes with two O donors, such as $[Ru(bpy)_2(OH_2)_2]^{2+}$ and O-$[Ru(bpy)_2(OSO)]^+$, indicating the formation of the O-bonded isomer.[25,26,69] The reaction is depicted in Scheme 1. What is notable is that despite differences in the S-bonded absorption maxima, the O-bonded maxima are essentially the same for all three complexes. This suggests that the electronic structure of the S-bonded isomer is more sensitive to substituent effects than the O-bonded isomer. The minimal variation of the O-bonded $Ru^{3+/2+}$ reduction potentials (Table 1) further support this conclusion.

Quantum yields of isomerization were collected and were relatively large for all complexes indicating a rapid rate of isomerization (Table 2).[31] Comparing the R = Bn, Nap, and Me complexes (R = Me, $\Phi_{s\rightarrow o}$= 0.45), there is a trend of decreasing quantum yield with bulkier substituents. Comparing the R = BnF_5 and Bn complexes, the more electron-withdrawing BnF_5 group results in a higher quantum yield of isomerization. These results indicate that the efficiency of isomerization is affected by both steric and electronic factors.

Transient absorption spectroscopy was employed to determine the kinetics of phototriggered isomerization. Selected time traces from the transient absorption spectra for S-$[Ru(bpy)_2(OSOBnF_5)]^+$ are shown in Figure 2. The initial traces (red) feature a bleach near 450 nm corresponding to the depletion of the ground state MLCT absorption, concomitant with a broad absorption at longer wavelengths which are attributed to the ligand-to-metal charge transfer (LMCT) transition from the neutral bpy to the Ru^{3+} center and a $\pi^*\rightarrow\pi^*$ transition arising from the reduced bpy. These features are characteristic of a thermally relaxed ^{3}MLCT excited state.[51−53,70−75] This state is achieved within approximately 1 ps. Subsequent traces show a decay in these features as well as a positive absorbance growing in at 500 nm. In the last time trace (blue), the broad long wavelength absorbance has decayed back to zero and only the absorbance feature centered at 500 nm remains. This spectrum qualitatively agrees with the difference between the S-bonded and O-bonded ground state absorption spectra (Figure 2, inset). Due to an approximate isosbestic point as well as a lack of a bleach feature near 500 nm, which would be indicative of an O-bonded ^{3}MLCT excited state, the transient absorption data suggest that isomerization proceeds directly from a S-bonded ^{3}MLCT state to the O-bonded ^{1}GS. Transient absorption data for R = Bn and Nap complexes are qualitatively similar (Supporting Information). Such a transition requires not only significant changes in nuclear coordinates but also a change in spin state. These multidimensional reaction coordinates typically occur at conical intersections and are thus termed nonadiabatic.[45]

Kinetic analysis of the transient absorption data for the R = BnF_5 complex (Figure 2b) produces a rate constant k_1 of 3.7 (±0.5) × 10^{10} s^{-1}. In accord with a nonadiabatic mechanism, this rate corresponds to the decay from the thermally relaxed S-bonded ^{3}MLCT state to both the S-bonded and O-bonded ground states, k_s and $k_{s\rightarrow o}$, respectively. Thus, for the R = BnF_5 complex with a quantum yield of 0.32, the rate constant of

(69) Juris, A.; Balzani, V.; Barigelletti, F.; Campagna, S.; Belser, P.; Von Zelewsky, A. *Coord. Chem. Rev.* **1988**, *84*, 85–277.
(70) Bhasikuttan, A. C.; Suzuki, M.; Nakashima, S.; Okada, T. *J. Am. Chem. Soc.* **2002**, *124*, 8398–8405.
(71) Curtright, A. E.; McCusker, J. K. *J. Phys. Chem. A* **1999**, *103*, 7032–7041.
(72) McFarland, S. A.; Lee, F. S.; Cheng, K. A. W. Y.; Cozens, F. L.; Schepp, N. P. *J. Am. Chem. Soc.* **2005**, *127*, 7065–7070.
(73) Ramakrishna, G.; Jose, D. A.; Kumar, D. K.; Das, A.; Palit, D. K.; Ghosh, H. N. *J. Phys. Chem. B* **2006**, *110*, 10197–10203.
(74) Wallin, S.; Davidsson, J.; Modin, J.; Hammarstrom, L. *J. Phys. Chem. A* **2005**, *109*, 4697–4704.
(75) Yeh, A. T.; Shank, C. V.; McCusker, J. K. *Science* **2000**, *289*, 935–938.

Table 2. Kinetic Results for $[Ru(bpy)_2(OSOR)]^+$

	R		
	Bn	Nap	BnF_5
$\Phi_{s\rightarrow o}$	0.22	0.16	0.32
k_1 (S-bonded), s^{-1}	1.56×10^{10}	1.42×10^{10}	3.7×10^{10}
$k_{s\rightarrow o}$, s^{-1} ($\tau_{s\rightarrow o}$, ps)	3.43×10^9 (291)	2.27×10^9 (427)	1.2×10^{10} (84)
k_2, k_3 (O-bonded), s^{-1}	8.6×10^{10}	8.3×10^{10}	1.2×10^{11}
	5.0×10^9	4.8×10^9	5.9×10^9
k_4, k_5 (thermal, 30 °C), s^{-1}	$5.74\ (\pm 0.06) \times 10^{-4}$	$5.98\ (\pm 0.04) \times 10^{-4}$	$3.32\ (\pm 0.12) \times 10^{-4}$
	$3.08\ (\pm 0.10) \times 10^{-6}$	$4.66\ (\pm 0.09) \times 10^{-6}$	$4.13\ (\pm 0.19) \times 10^{-5}$

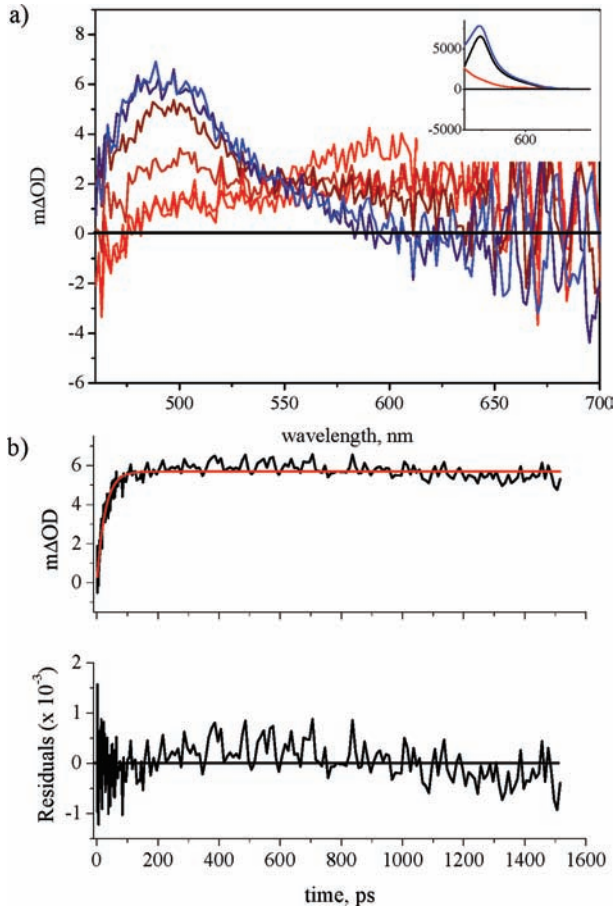

Figure 2. (a) Picosecond transient absorption of S-bonded $[Ru(bpy)_2(OSOBnF_5)]^+$ in methanol. Starting in red time traces are: 5.0, 10.2, 20.3, 50.7, 100.3, 495.3 ps. Inset: Absorption spectra, ϵ (M^{-1} cm^{-1}) vs wavelength (nm) of S-bonded (red), O-bonded (blue) and O−S (black). (b) Kinetic trace at 500 nm yields $\tau_{s\rightarrow o} = 84$ ps.

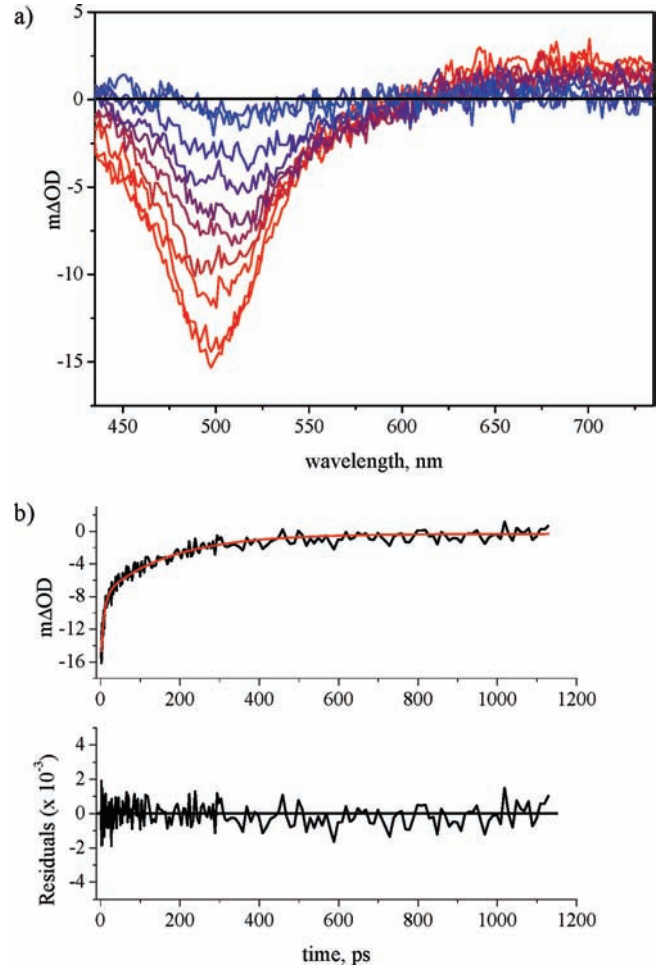

Figure 3. (a) Picosecond transient absorption of O-bonded $[Ru(bpy)_2(OSOBnF_5)]^+$ in methanol. Starting in red time traces are: 1.0, 2.0, 5.0, 10.3, 20.4, 50.4, 101.1, 203.0, 508.0, 1008 ps. (b) Kinetic trace at 500 nm yields biexponential decay with time constants of 8.4 and 170 ps.

isomerization ($k_{s\rightarrow o}$) is 1.2×10^{10} s^{-1} yielding a time constant for isomerization ($\tau_{s\rightarrow o}$) of 84 (±11) ps. The isomerization time constants for the R = Bn and Nap complexes are 291 (±5) ps and 427 (±24) ps, respectively. The k_1 values of both of the R = Bn and Nap complexes are similar (Table 2) and agree well with that of the R = Me complex (1.48×10^{10} s^{-1}).[26] Thus the slower rate of isomerization arises mainly from the smaller quantum yields of isomerization. Comparatively, the k_1 value for the R = BnF_5 complex is faster by a factor of ~2.5 in addition to a quantum yield that is greater than both of the R = Bn and Nap complexes. Despite the greater quantum yield for the R = Me complex (0.45), the k_1 value is sufficiently fast enough for R = BnF_5 that $\tau_{s\rightarrow o}$ is faster (84 ps compared to 150 ps). The rate of isomerization for R = BnF_5 is the fastest we have observed for any ruthenium sulfoxide complex and is comparable to the rate of isomerization in stilbene, which has a time constant of 42 ps[76] in methanol and a rate constant of $\sim 10^{10}$ s^{-1} in other solvents.[77] Fast isomerization rates indicate an efficient conversion of photonic energy into potential energy for photochemical bond cleavage and formation. This is presumably due in part to the large nuclear displacement exhibited by these complexes.

The O-bonded transient absorption spectra for the R = BnF_5 complex are shown in Figure 3. The initial traces exhibit a bleach feature centered at 500 nm as well as a broad positive absorption at longer wavelengths to the limit of detection. We

(76) Courtney, S. H.; Balk, M. W.; Philips, L. A.; Webb, S. P.; Yang, D.; Levy, D. H.; Fleming, G. R. *J. Chem. Phys.* **1988**, *89*, 6697–6707.
(77) Waldeck, D. H. *Chem. Rev.* **1991**, *91*, 415–436.

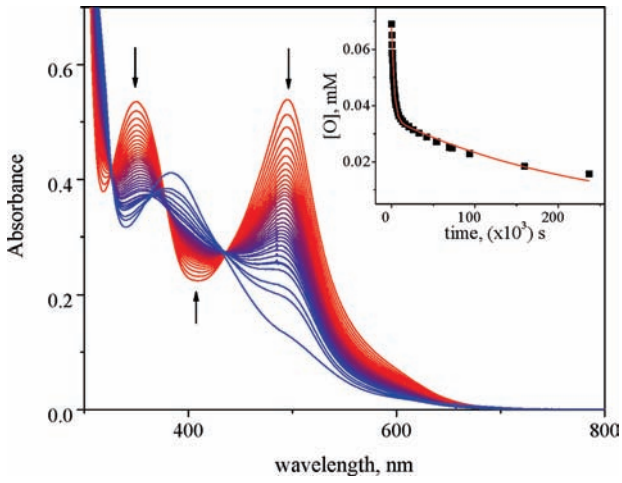

Figure 4. Thermal reversion of $[Ru(bpy)_2(OSOBnF_5)]^+$ in methanol at 30 °C. Arrows indicate reaction progression from O-bonded (red) to S-bonded (blue). Inset: Kinetics fit to biexponential decay with rate constants of 3.32 ($\pm$0.12) $\times$ 10^{-4} s^{-1} and 4.13 ($\pm$0.19) $\times$ 10^{-5} s^{-1}.

have interpreted this as the formation of the thermally relaxed O-bonded ^{3}MLCT within the first ~1 ps (red trace). Unlike the S-bonded complex, further time traces show a spectrum indistinguishable from the zero line (blue trace), which is indicative of decay to only the O-bonded ground state surface. The decay is biexponential with time constants of $\tau_2 = \sim$10 ps and $\tau_3 = \sim$ 200 ps (Figure 3b). As we have described previously, the longer time constant is consistent with the decay of the O-bonded ^{3}MLCT to the ground state for other complexes, and the shorter time constant may be attributed to some minor rearrangement prior to decay to the ground state.[26]

The proposed nonadiabatic isomerization mechanism requires that the thermally relaxed S-bonded excited state geometry is significantly displaced from the ground state. This is consistent with the broad absorption spectra for these complexes. A reasonable structure is an η^2-type or asymmetric η^2 structure. To our knowledge, this bonding has not been observed in any sulfoxide complex, although it has been observed in the metastable states of complexes containing SO_2.[78−80] Briefly, irradiation of single crystals of $[Ru(NH_3)_4(L)(SO_2)]^{2+}$ (L = NH_3 or H_2O) yields both η^2-SO_2 and O-bonded SO_2 metastable coordination modes. Clearly, the transition states for these reactions must involve some asymmetric η^2-type bonding.

Consistent with other complexes of this class, the metastable O-bonded isomers were found to thermally revert in methanol solution at room temperature (Figure 4). In accord with $[Ru(bpy)_2(OSO)]^+$, the reversion kinetics exhibit biexponential behavior (rate constants: $k_4 \sim 10^{-4}$ s^{-1}, $k_5 \sim 10^{-6}$ s^{-1}, inset Figure 2); however, unlike this complex, there are two sets of isosbestic points. These results are consistent with the interpretation of two O-bonded isomers found electrochemically. While these may be diastereomers, it is difficult to explain the disparity in rate constants. Thus we propose that the fast rate is some molecular rearrangement preceding O→S isomerization. The rate constants of thermal reversion at 30 °C in methanol are listed in Table 2. As for other chelating sulfoxide complexes[25,28] the rate of thermal reversion for these complexes is much slower than previously studied dmso complexes[29,30] and is attributed to fewer degrees of freedom imposed by the chelating sulfoxide ligand. Comparing R = Bn and Nap complexes, k_4 values are similar whereas for k_5 values the R = Nap complex is faster. This is counterintuitive since the sterically bulkier group would be expected to inhibit the thermal reversion and proceed at a slower rate. Comparison of R = Bn and BnF_5 complexes is not straightforward. The k_4 value is greater in the R = Bn complex, but the k_5 value is greater in the R = BnF_5 complex. This suggests there is a more complicated electronic effect on the rate of thermal reversion parameters. Further studies will elucidate these effects.

Table 3. 77 K Corrected Emission Spectra Fitting Parameters

Complex	E_0, cm^{-1}	$h\nu_m$, cm^{-1}	$h\nu_l$, cm^{-1}	S_m	S_l	*fwhm*, cm^{-1}
$[Ru(bpy)_3]^{2+}$	17 500	1400	400	0.8	1.0	600
$[Ru(bpy)_2(OSOBn)]^+$	17 200	1150	–	1.4	–	1450
$[Ru(bpy)_2(OSONap)]^+$	17 200	1150	–	1.4	–	1450
$[Ru(bpy)_2(OSOBnF_5)]^+$	17 300	1300	–	1.2	–	1600

The 77 K corrected emission spectra provide further evidence of a large displacement between ground state and thermally relaxed excited state structures. The sulfoxide complexes all exhibit particularly large Stokes shifts (7890 cm^{-1} R = Bn, 7760 cm^{-1} R = Nap, 8290 cm^{-1} R = BnF_5). These shifts are significantly larger than those observed for the model complex $[Ru(bpy)_3]^{2+}$ (~ 6000 cm^{-1}, H_2O)[81] as well as the corresponding thioether complexes (5360 cm^{-1} R = Bn, 5460 cm^{-1} R = Nap, 5680 cm^{-1} R = BnF_5).

Corrected emission spectra were normalized and fit using eq 3[82] (Figure 1; Supporting Information) to obtain values of E_0, *fwhm*, S_m, and S_l, in which E_0 and *fwhm* are defined as in eq 2, and S_m and S_l are the electron-vibrational coupling constants or Huang−Rhys parameters for the medium frequency, $h\nu_m$, and low frequency, $h\nu_l$, modes, respectively. Values for $[Ru(bpy)_3]^{2+}$ were found to be in close agreement with previously reported values.[83] The spectrum was fit to two modes, one medium frequency intraligand mode (1400 cm^{-1}) and one low frequency metal−ligand mode (400 cm^{-1}). Unlike the 200 K spectrum, the 77 K spectrum of $[Ru(bpy)_3]^{2+}$ requires the inclusion of a low energy vibrational mode to adequately model the data.[83,84] In contrast, the 77 K spectra for $[Ru(bpy)_2(OSOR)]^+$ complexes were fit using only one vibrational mode and Huang−Rhys parameter (Table 3). The most notable feature is that the *fwhm* of these complexes are significantly larger than that for $[Ru(bpy)_3]^{2+}$. In accord with the absorption spectra, a large *fwhm* value is indicative of substantial nuclear displacement between the equilibrium ground state and ^{3}MLCT state geometries. The medium frequency mode ($h\nu_m$) has shifted to lower energy from 1400 cm^{-1} to 1150−1300 cm^{-1}, which is in relatively close agreement with the ν(S═O) stretch obtained by IR spectroscopy (Table 1). We interpret the shift to lower energy of the medium frequency mode as inclusion of the S═O stretch as a significant

(78) Bowes, K. F.; Cole, J. M.; Husheer, S. L. G.; Raithby, P. R.; Savarese, T. L.; Sparkes, H. A.; Teat, S. J.; Warren, J. E. *Chem. Commun.* **2006**, 2448–2450.
(79) Kovalevsky, A. Y.; Bagley, K. A.; Cole, J. M.; Coppens, P. *Inorg. Chem.* **2003**, *42*, 140–147.
(80) Kovalevsky, A. Y.; Bagley, K. A.; Coppens, P. *J. Am. Chem. Soc.* **2002**, *124*, 9241–9248.
(81) Yoon, S.; Kukura, P.; Stuart, C. M.; Mathies, R. A. *Mol. Phys.* **2006**, *104*, 1275–1282.
(82) Barqawi, K. R.; Murtaza, Z.; Meyer, T. J. *J. Phys. Chem.* **1991**, *95*, 47–50.
(83) Caspar, J. V.; Westmoreland, T. D.; Allen, G. H.; Bradley, P. G.; Meyer, T. J.; Woodruff, W. H. *J. Am. Chem. Soc.* **1984**, *106*, 3492–3500.
(84) Caspar, J. V.; Meyer, T. J. *Inorg. Chem.* **1983**, *22*, 2444–2453.

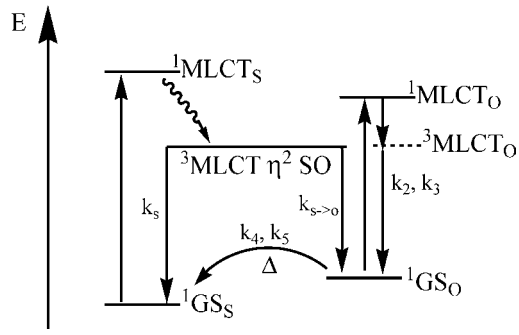

Figure 5. Modified Jablonksi type diagram for $[Ru(bpy)_2(OSOR)]^+$. ^1GS_S and ^1GS_O are the S-bonded and O-bonded ground states. $^1MLCT_S$ and $^1MLCT_O$ are S-bonded and O-bonded excited states. The O-bonded ^{3}MLCT state is denoted as a dashed line since the relative energy is not known.

component of excited state deactivation. Due to the poor vibrational resolution in the spectrum, we cannot distinguish the relative contributions of these modes. The S_m values are also increased relative to $[Ru(bpy)_3]^{2+}$. This suggests greater coupling between the electronic states and medium frequency vibrational mode, again indicating that the S═O stretching mode is strongly coupled to excited state relaxation.

$$I_\nu = \sum_{m=0}^{5}\sum_{l=0}^{15}\left(\frac{E_0 - mh\nu_m - lh\nu_l}{E_0}\right)^3 \frac{S_m^m S_l^l \exp\left[-4\ln 2\cdot\left(\frac{\nu - E_0 + mh\nu_m + lh\nu_l}{fwhm}\right)^2\right]}{m!\cdot l!} \quad (3)$$

However, the results of the emission and absorption spectral data are not directly comparable because the absorption spectrum quantifies the distortion energy between the ^{1}GS and ^{1}MLCT potential energy surfaces, whereas the emission spectrum quantifies the distortion energy between the thermally relaxed ^{3}MLCT and ^{1}GS potential energy surfaces. Furthermore, there are significant differences due to solvent/matrix and temperature (300 K compared to 77 K). The *fwhm* values of the room temperature absorption spectra are a factor of 4−5 *larger* than those for the corresponding 77 K emission spectra. Thus it appears that the potential energy surfaces and distortion energy between the ground state and ^{3}MLCT are strongly temperature and solvent dependent, as is expected for a nonadiabatic isomerization.

The results presented herein are summarized in Figure 5. The difference between ^1GS_S and ^1GS_O is determined electrochemically. Following absorption of a photon by ^1GS_S to form $^1MLCT_S$, internal conversion, intersystem conversion, and intramolecular vibrational relaxation occur to yield a ^{3}MLCT-η^2 SO state. Relaxation from this state proceeds back to ^1GS_S with a rate constant of k_s and to ^1GS_O with the rate constant of isomerization, $k_{s\rightarrow o}$. The sum of these two terms is k_1 as listed in Table 2. Following excitation to $^1MLCT_O$ from ^1GS_O, relaxation occurs biexponentially with rate constants k_2 and k_3 (Table 2). ^1GS_O thermally reverts to ^1GS_S with rate constants k_4 and k_5 (Table 2).

The ^{3}MLCT state is formed within ∼1 ps with substantial nuclear displacement from the initially produced ^{1}MLCT state. Our kinetic analysis demonstrates that S→O isomerization occurs rapidly and efficiently on a picosecond time scale. While our spectroscopic analysis does not reveal a clear relationship between distortion energy and isomerization reactivity, it does show significant excited state mixing from low energy metal−ligand and S═O vibrational modes with the electronic transitions. We propose that S→O isomerization or surface hopping is enhanced by this distortion and occurs through a conical intersection formed from a multidimensional reaction coordinate. Future studies will further investigate these relationships.

Acknowledgment. We thank Dr. Aaron Rachford for helpful discussions in preparing this manuscript. We are grateful to Dr. Evgeny Danilov for experimental assistance at the Ohio Laboratory for Kinetic Spectrometry at BGSU and for access to the femtosecond transient absorption spectrometer employed in these studies. J.J.R. acknowledges NSF (CHE 0809669), Ohio University, Condensed Matter and Surface Science (CMSS), and the Nano-BioTechnology Initiative (NBTI) for funding. B.A.M. recognizes NDSEG for a fellowship.

Supporting Information Available: Transient absorption spectra of S-bonded and O-bonded $[Ru(bpy)_2(OSOBn)]^+$ and $[Ru(bpy)_2(OSONap)]^+$ and associated kinetic traces, 77 K emission spectra with calculated fits of $[Ru(bpy)_3]^{2+}$, S-$[Ru(bpy)_2(OSOBn)]^+$, and S-$[Ru(bpy)_2(OSONap)]^+$. This material is available free of charge via the Internet at http://pubs.acs.org.

JA9099399